Vietnam Journal of Science and Technology ***62*** *(3) (2024) 577-587*

doi:10.15625/2525-2518/17140

Synthesis of nickel-doped $BiVO_4$ materials by hydrothermal method and evaluation of their photocatalytic ability to decompose methylene blue under visible light

Van Thinh Pham[1, 2], Bach Tuyet T. Dao[3], Thi Kim Ngan Tran[4], Ngoc Quyen Tran[1, 5], Long Giang Bach[1, 4, *]

[1]*Graduate University of Science and Technology, Vietnam Academy of Science and Technology, 18 Hoang Quoc Viet, Cau Giay, Hanoi, Viet Nam*

[2]*Faculty of Food Science and Technology, Ho Chi Minh City University of Food Industry, 140 Le Trong Tan, Tan Phu District, Ho Chi Minh City, Viet Nam*

[3]*Faculty of Chemical Technology, Ho Chi Minh City University of Food Industry, 140 Le Trong Tan, Tan Phu District, Ho Chi Minh City, Viet Nam*

[4]*Institute of Applied Technology and Sustainable Development, Nguyen Tat Thanh University, 01 Vo Chi Cong Street, District 9, Thu Duc Ciy, Ho Chi Minh City, Ho Chi Minh City, Viet Nam*

[5]*Institute of Applied Materials Science, Vietnam Academy of Science and Technology, 1B TL29 Street, Thanh Loc Ward, Distric 12, Ho Chi Minh City, Viet Nam*

[*]Emails: *blgiang@ntt.edu.vn*

Received: 16 May 2022; Accepted for publication: 5 September 2022

Abstract. Ni-doped $BiVO_4$ photocatalysts were successfully synthesized by hydrothermal method. The catalytic samples were characterized by scanning electron microscopy (SEM), UV-vis diffuse reflection spectroscopy (DRS), photoluminescence spectroscopy (PL) and X-ray diffraction (XRD). Based on the results of PL spectrum analysis, the electron-hole recombination phenomenon is limited by the presence of the second metal Ni in the structure at Bi^{3+} sites. The catalyst materials at the Ni doping ratios all have the monoclinic-scheelite $BiVO_4$ structure as shown by the XRD and Raman methods. The photocatalytic ability of methyl blue (MB) on the Ni/$BiVO_4$ catalyst was studied under visible light irradiation in order to contribute to reducing the current environmental pollution problem. The removal efficiency of MB varies with the doping ratio of Ni/$BiVO_4$, reaching the highest decomposition efficiency of 84.77 % in the 5 % mol Ni sample, which is 30 % higher than that of the $BiVO_4$ sample. The $BiVO_4$ material modified with Ni giving a high photocatalytic efficiency of organic pigment decomposition under visible light indicates the potential improvement in the efficiency of a material for existing applications and exploit many new applications in the future.

Keywords: $BiVO_4$, photocatalytic, methylene blue, hydrothermal.

Classification numbers: 5.5.3

1. INTRODUCTION

Nowadays, along with the rapid development of the industries, the issue of environmental pollution is increasing at alarming rate, especially water pollution. In particular, the textile industry is one of the industries that discharges a significant amount of hazardous waste into the water environment, causing pollution to the water resources and degrading the water quality. Recently, a new advanced oxidation method has been developed for the treatment of textile and dyeing wastewater. This method involves the use of catalysts as semiconductors to generate HO• radicals with very strong oxidizing ability that can decompose most toxic organic substances under lighting conditions [1 - 3]. $BiVO_4$ material is considered as one of the new generation materials for the decomposition of pollutant compounds as it can absorb the visible light region (gap energy is 2.4 eV). However, the actual efficiency achieved by this material remains far from expectations owing to the poor electron-hole separation efficiency. Research efforts have focused on improving the electron-hole separation efficiency, including (1) controlling the crystal structure, crystallite morphology and crystal face, (2) p-n bond formation, and (3) forming the monoclinic-tetragonal polyphasic structure of $BiVO_4$ [4, 5]. To this end, many studies have been reported. Chhabilal *et al*. (2017) carried out experiments to remove water contaminants such as Escherichia coli (bacteria), green tides (phytoplankton), and ibuprofen (pharmaceutical) using a Ni-doped BiVO4 catalyst synthesized by microwave-hydrothermal method [ref.?]. The photocatalytic efficiency is determined by the Ni doping in the position of the BiVO4 lattice, the separation of electron-hole pairs increases and prevents the recombination of the carriers by the intermediate energy state. Specifically, the photocatalytic degradation efficiency of green tides (70 %, 60 minutes), *E. coli* (92 %, 5 hours) and IBP (80 %, 90 minutes) under visible light [6]. M - $BiVO_4$ catalyst materials (M = Ag, Co and Ni) were successfully synthesized based on heteronuclear complex precursors by Bin Zhou *et al.* (2021). The photocatalyst M - $BiVO_4$ decomposes almost 90 % of 2,4-dichlorophenol and 85 % of methylene blue under visible light [7].

Obregon *et al*. (2012) [8] successfully prepared needle-shaped $BiVO_4$ by hydrothermal method without using surfactants, mainly depends on pH values, type of precipitating agent, temperature and hydrothermal time. $BiVO_4$ material with monoclinic-tetragonal heterostructure is able to effectively improve the photochemical activity. Tan *et al*. (2013) [9] showed that $BiVO_4$ with monoclinic-tetragonal heterostructure prepared by hydrothermal method hydrothermal method based on the change of pH value, exhibited much higher activity than the monoclinic form (m-s $BiVO_4$, t-s $BiVO_4$), under the effect of UV light or visible light. In addition, Usai *et al*. (2013) [10] reported another synthesis method by which $BiVO_4$ with monoclinic-tetragonal heterostructure can be prepared by modifications with yttrium.

The $BiVO_4$ photocatalyst has proven to be a promising material for a variety of applications, including the optical degradation of dyes and the use of sunlight in an eco-friendly photocatalysis process [11–14]. However, $BiVO_4$ has limitations in the process of recombination of the dominant fast electrons and holes, resulting in the degradation of the photochemical activity of the material. This problem has been improved by a number of measures such as controlling the crystal structure (research and synthesis of s-m $BiVO_4$ structural materials or m-t $BiVO_4$ heterostructures), size control and $BiVO_4$ crystal morphology (research and synthesis of $BiVO_4$ materials with micro-nano size, sheet, fibrous, tubular, spherical, star shape, etc.), and modification of $BiVO_4$ by doping metals (Au, Ag, Fe, Co, Ni, Cu, Ce), composite materials based on $BiVO_4$ [15 - 18].

Therefore, in this study, we focused on the modification of $BiVO_4$ and investigated the synthesis of a new photocatalyst that can use visible light instead of UV light with high efficiency at a reasonable cost and can be applied in many fields, especially in environmental remediation. With the attempt of producing the materials with improved photocatalytic activity using a simple and low-cost process, the method of synthesizing $BiVO_4$ catalyst by hydrothermal method is feasible and potential for industrial-scaled development. The composites were structurally characterized by XRD, SEM and UV-Vis DRS methods from which methylene blue dye removal was applied.

2. MATERIALS AND METHODS

2.1. Chemicals

Bismuth(III) nitrate pentahydrate (98 %), NH_4VO_3 (99 %) and methylene blue were purchased from Sigma-Aldrich (St. Louis, MO, USA). $Ni(NO_3)_2.6H_2O$ (98 %), NaOH, HNO_3 from Xilong Chemical Co., Ltd. (Guangzhou, China).

2.2. Preparation of Catalysts

The process of synthesizing the original $BiVO_4$ and Ni-doped $BiVO_4$ with different ratios by hydrothermal method was based on the study of Anjali Athawale *et al*. [19]. Briefly, $Bi(NO_3)_3.5H_2O$ and $Ni(NO_3)_2.6H_2O$ were dissolved in 20 ml of solvent. 2 M HNO_3, was then stirred well for 30 min to form solution A. NH_4VO_3 was dissolved in 40 ml of 0.3 M NaOH solution and stirred well for 30 min to form solution B. The solution B was slowly mixed with solution A and the mixture was continued stirring for 30 min. Then, the pH of the mixture was adjusted to 10 by using 4 M NaOH and stirred well for 30 min to stabilize the pH. Distilled water was added to the mixture to obtain a total volume of 80 ml. The mixture was placed in teflon and heated to 180 ºC for 24 h. The hydrothermal mixture was washed by centrifugation with distilled water several times until pH 7 and dried at 80 ºC for 24 h. After drying, the material in powder form was calcined at 300 °C for 2 h.

2.3. Characterization of catalysts

The X diffraction (XRD) patterns were measured on a Bruker D8 advance. UV-Vis DRS spectra were measured on a Shimadzu UV-2450 instrument. SEM images of the material samples after synthesis were investigated on the JSM 7401F device of Jeol. Photoluminescence (PL) spectra were performed using excitation light with wavelength 315 nm, on an F-4500 Spectro-fluorometer (Hitachi, Japan).

2.4. Photocatalytic reaction

The photocatalytic activity of the materials was evaluated on the decomposition reaction of the organic pigment Methylene Blue (MB) using visible light. The procedure to evaluate the photocatalytic activity in the color degradation reaction of MB under visible light of the material samples was carried out by dissolving the catalytic samples (0.05 g) into 100 ml of solvent in a 250 ml double-layer glass beaker. The solution was stirred in the dark for 60 min to achieve adsorption equilibrium, then illuminated (60 W LED) and sampled over time. The sample was then centrifuged (5000 rpm/10 min) to separate the material from the color. After centrifugation,

the sample was collected and measured on a UV-Vis machine (the Thermo brand) to determine the light absorption.

3. RESULTS AND DISCUSSION

Ni-doped $BiVO_4$ samples were synthesized with different Ni/Bi^{3+} ratios. As shown in Figure 1, as the doping ratio increases, the yellow color of the material becomes less intense. At low doping ratio (2 % to 5 %), the material appears in a dark yellow color, yet when the doping ratio is increased from 10 % to 30 % mol Ni, the color of the material turns into light blue.

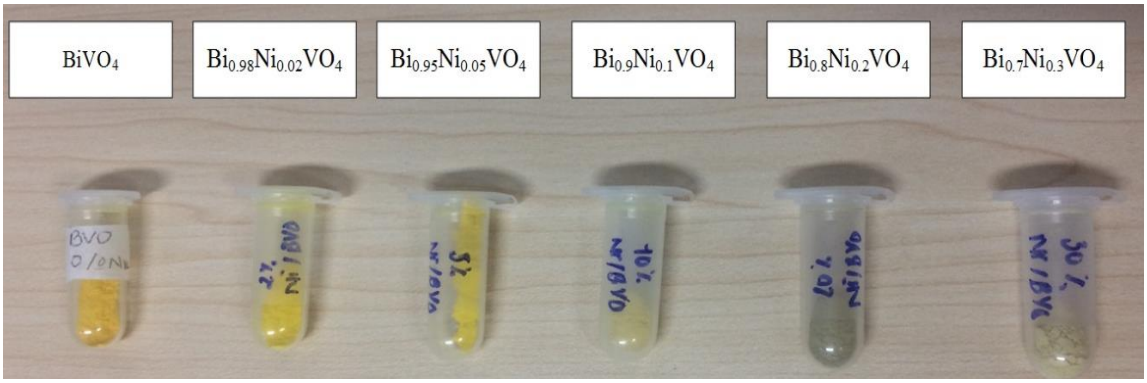

Figure 1. Real images of Ni-doped $BiVO_4$ samples with Ni/Bi^{3+} ratio change.

To investigate the effect of the Ni-doping ratio on the crystalline phase formation of $BiVO_4$, the crystal structure of the undoped and Ni-doped $BiVO_4$ samples was determined by XRD. The XRD measurement results show that the XRD pattern of undoped $BiVO_4$ with diffraction peaks on the XRD pattern is consistent with the crystal structure of monoclinic scheelite with the characteristic strong diffraction peak at angle $2\theta = 29.4°$ (crystal face (121)) and weak diffraction peaks separated at $2\theta = 19.1°$; 30.5° and 47.6°, which is consistent with JPCDS standard card number 14-0688 in the data bank (Figure 2). For the XRD pattern of the Ni-doped $BiVO_4$ samples, when changing the Ni/Bi^{3+} ratio, the Ni samples that were doped at different molar ratios (from 2 % to 30 %) exhibited no phase change in general. At the ratios from 2 % to 10 % mol, the samples at this ratio have characteristic diffraction peaks of m-s $BiVO_4$ crystal structure at the $2\theta = 19.3°$; 29.4°; 30.7° and 47.8°, conforming to JPCDS standard card number 14-0688. For the Ni-doped $BiVO_4$ sample, when increasing the molar ratio of Ni/Bi^{3+} from 20 % mol to 30 % mol, the characteristic diffraction peaks of the s-m $BiVO_4$ crystal structure at $2\theta = 19.3°$; 30.5° (crystal face (011); (040)) were observed, similarly to the study published by Chhabilal *et al.* (2017) [6]. In addition, some strange peaks appeared such as the peak of α Bi_2O_3 phase at position $2\theta = 28.1°$ (crystal face (1 2 0)), the peak of phase β-Bi_2O_3 at position $2\theta = 28.9°$ (crystal face (201)), and the peak of phase V_2O_5 at positions $2\theta = 25.2°$; 34.6 (crystal face (110)); (130)). The peak intensities of α-Bi_2O_3 and β-Bi_2O_3 are clearly shown in Figure 2. The formation of the above characteristic peaks depends mainly on the hydrothermal method, which plays an important role in the formation of the β phase. On the other hand, it is found that the β-Bi_2O_3 sample has wider diffraction peaks than the α phase samples. The ionic radius of Bi^{3+} (0.103 nm) is larger than Ni^{2+} (0.069 nm), so it is difficult for Ni^{2+}, to penetrate into the structure of BiVO4, so the nickel element is deposited on the surface of BiVO4 particles in the form of oxide. The incorporation of Ni^{2+} in the lattice of BiVO4, can be caused by the substitution of V^{5+}

(0.059 nm) with Ni^{2+} (0.069 nm), the diffraction peak is widened due to the increased Ni doping concentration, this shows that the crystallite size decreases, the intensity decreases with increasing doping concentration [20].

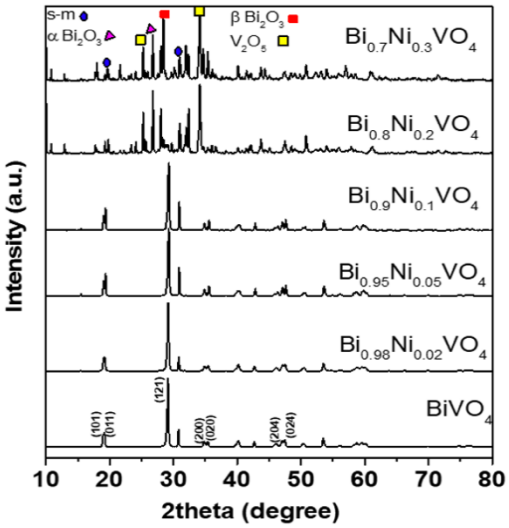

Figure 2. XRD patterns of the Ni-doped $BiVO_4$ sample with the Ni/Bi^{3+} ratio changed.

Figure 3 is the scanning electron microscope (SEM) image of the Ni-doped $BiVO_4$ sample with various Ni/Bi^{3+} ratios. The undoped $BiVO_4$ sample has a heterogeneous surface morphology with spherical crystallites of about 1-3 µm in size. For the Ni-doped samples with different Ni-doping ratios from 2 % to 30 %, the crystallites were of small sizes and heterogeneous shapes. Specifically, the sample (5 %) $Bi_{0.95}Ni_{0.05}VO_4$ has the form of stacked pellets with a crystallite size of about 1 - 2 µm.

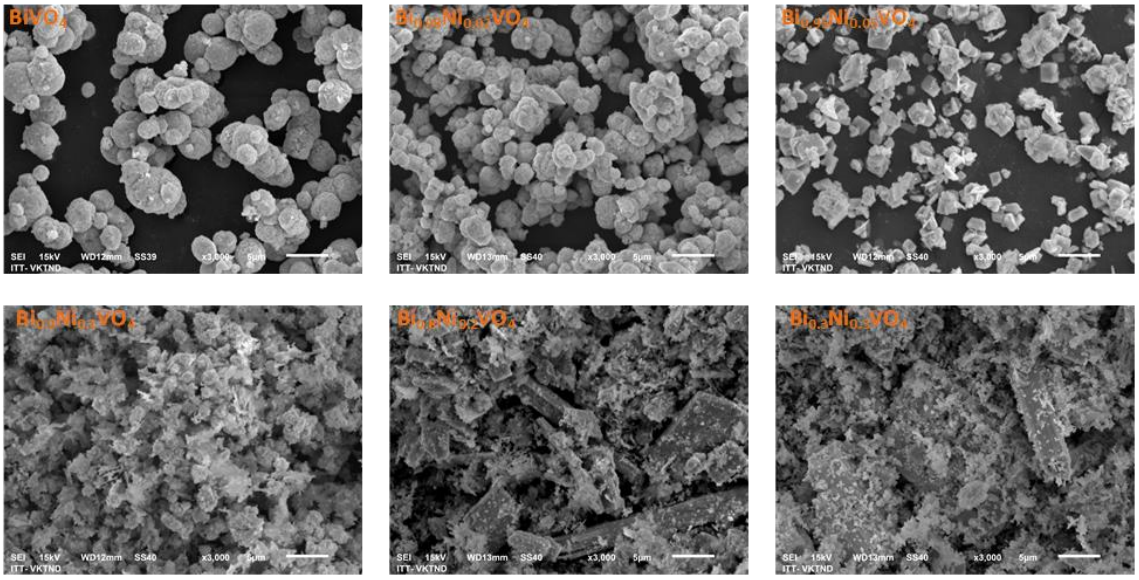

Figure 3. SEM image of the Ni-doped $BiVO_4$ sample with changes in the Ni/Bi^{3+} ratio.

The ability to absorb light in the short-wavelength (UV) and long-wavelength regions (visible light region) of the material samples was studied by UV-Vis DRS. Results of the undoped and Ni-doped $BiVO_4$ sample at the Bi^{3+} position at the wavelength range from 300 to 800 nm are shown in Figure 4. In general, the samples absorb in the visible light region. Specifically, the undoped $BiVO_4$ sample exhibits absorption in the visible light region and extends to a wavelength of about 550 nm, which is consistent with the results of previous studies [10]. The Ni metal-doped samples have an increased absorption in the visible light region and extend to a wavelength of about 550 nm. The band gap energy of the catalyst material (E_g) is determined by the line tangent to the graph of the Kubelka–Munk function $[F(R\infty)hv]1/2$ with the corresponding photon energy hv. The band gap energies of the material samples range from 2.32 eV - 2.36 eV (Table 1), which is consistent with the results of previous studies [10].

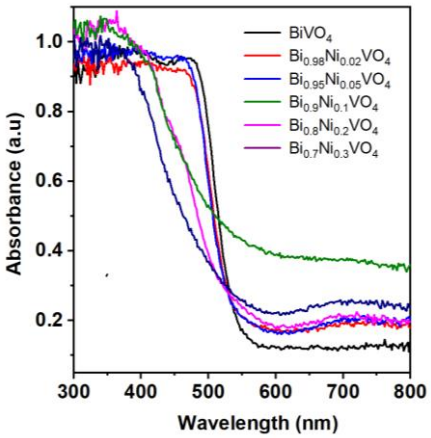

Figure 4. Absorption spectra of the undoped and Ni-doped $BiVO_4$ sample at the Bi position.

Table 1. Band gap energy of undoped and Ni-doped $BiVO_4$ samples at Bi position.

Materials	**E_g (eV)**
$BiVO_4$	2.32
(2 %) $Bi_{0.98}Ni_{0.02}VO_4$	2.3
(5 %) $Bi_{0.95}Ni_{0.05}VO_4$	2.31
(10 %) $Bi_{0.9}Ni_{0.1}VO_4$	2.33
(20 %) $Bi_{0.8}Ni_{0.2}VO_4$	2.35
(30 %) $Bi_{0.7}Ni_{0.3}VO_4$	2.36

To investigate the influence of the Ni-doping ratio on the luminescence of the materials, the luminescence ability of the undoped and Ni-doped $BiVO_4$ samples was determined by PL method. Low PL intensity generally indicates a higher separation efficiency of the photocatalyst charges, thus higher photocatalytic activity. The PL spectrum of the undoped and Ni-doped $BiVO_4$ sample at the Bi^{3+} position (specifically, sample (2 %) $Bi_{0.98}Ni_{0.02}VO_4$ and sample (5 %) $Bi_{0.95}Ni_{0.05}VO_4$) shown in Figure 5 demonstrated that when receiving the excitation light with wavelength 315 nm, only the $BiVO_4$ samples are luminescent at wavelengths from 400 nm to

500 nm, (2 %) $Bi_{0.98}Ni_{0.02}VO_4$ and sample (5 %) $Bi_{0.95}Ni_{0.05}VO_4$ samples are less luminescent at 400 nm to 500 nm. The samples of $BiVO_4$ without doping and without doping with Ni at the remaining Bi^{3+} positions showed similar results as the sample $Bi_{0.98}Ni_{0.02}VO_4$. This can be explained that the ability to recombine electrons with holes and generate energy in the form of light of the $BiVO_4$ sample is higher than that of the Ni-doped samples at the Bi^{3+} position. The PL intensity decreased in the order of: $BiVO_4$ > (2 %) $Bi_{0.98}Ni_{0.02}VO_4$ > (5 %) $Bi_{0.95}Ni_{0.05}VO_4$, which is opposite to the photocatalytic activity. Therefore, this result further confirms that (5 %) $Bi_{0.95}Ni_{0.05}VO_4$ sample has high catalytic activity.

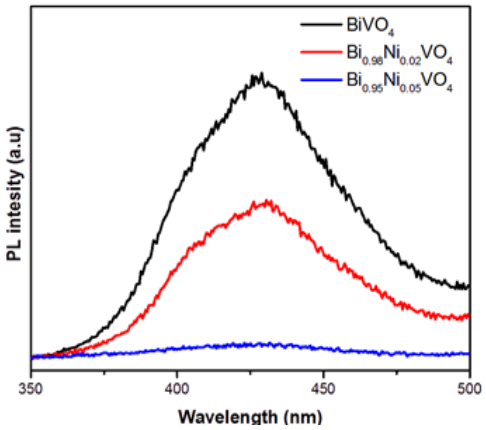

Figure 5. PL spectra of $BiVO_4$, (2 %) $Bi_{0.98}Ni_{0.02}VO_4$ and (5 %) $Bi_{0.95}Ni_{0.05}VO_4$ samples.

The influence of the doping ratio on the photocatalytic activity of the materials is shown in Figure 6 and summarized in Table 2. The results show that the undoped $BiVO_4$ sample upon exposure to darkness for 60 min has absorbed an amount of 7.5 of MB. Then upon light exposure for 3 h, the MB treatment efficiency reach 54.56 % (Figure 6A. For the Ni-doped $BiVO_4$ samples at the Bi^{3+} position, when increasing the Ni content from 2 % to 10 %, the MB treatment efficiency gradually increases and reaches the highest level in 5 % Ni-doped samples. Specifically, for the sample (5 %) $Bi_{0.95}Ni_{0.05}VO_4$ that has the highest photocatalytic activity, the MB treatment efficiency after 3 h of light exposure was 83.77%. However, as the content continued to increase from 20 % to 30 %, the MB processing efficiency would decrease sharply. In contrast, for the sample (30 %) $Bi_{0.7}Ni_{0.3}VO_4$ that has the lowest photocatalytic activity, the treatment efficiency is only 41.40 % after 3 h of illumination. For example, Sha Li *et al*. [21] showed the ability to remove rhodamine B (RhB) pigment in the presence of 0.75 % Ni in $BiVO_4$. Under visible light conditions, 96 % RhB was removed after 75 minutes, the efficiency is 52 % higher than BiVO4 catalyst. Therefore, the material achieves the highest MB treatment efficiency when being doped with 5 % molar ratio. The MB solution before and after treatments with (5 %) $Bi_{0.95}Ni_{0.05}VO_4$ material is shown in Figure 7.

According to the previous reports [22], when the pollutant is in the range of mM concentration, the photocatalytic oxidation of organic pollutants follows the first-order kinetic equation, thus the rate constant degree (k) is calculated for the photocatalytic degradation of MB under visible light irradiation by the following equation:

$$k = -\frac{1}{t}\ln\left(\frac{C}{C_0}\right)$$

where C_0 and C are the concentrations of MB when the reaction times are 0 and t, respectively.

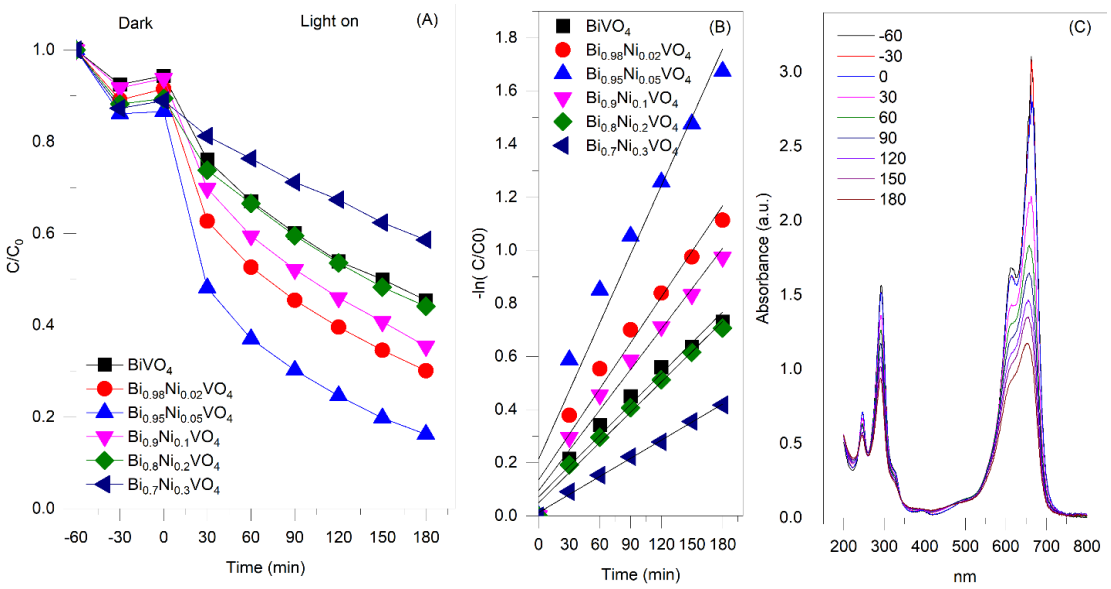

Figure 6. The photocatalytic activity of the undoped and Ni-doped $BiVO_4$ materials at the Bi^{3+} position in the MB (A) color degradation reaction; Kinetics of undoped and Ni-doped $BiVO_4$ materials at Bi^{3+} position in MB (B) color degradation reaction; UV-Vis absorption spectrum of MB solution illuminated with time catalyzed by (5 %) $Bi_{0.95}Ni_{0.05}VO_4$ (C).

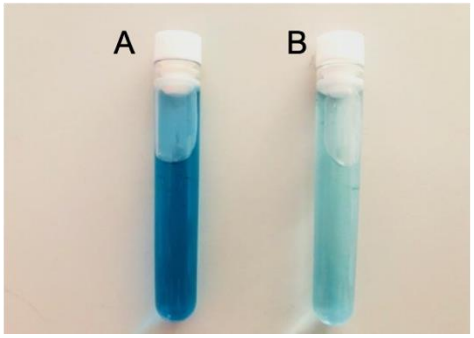

Figure 7. MB solution before (A) and after (B) the treatment with $Bi_{0.95}Ni_{0.05}VO_4$ material.

Table 2. Photocatalytic performance and kinetic results of undoped and Ni-doped $BiVO_4$ materials at Bi^{3+} position in MB color degradation reaction.

Materials	**Ni-doping ratio (%mol)**	**Treatment efficiency (%)**	**K**	**R^2**
$BiVO_4$	0	54.56	$3.87.10^{-3}$	0.96724
(2 %) $Bi_{0.98}Ni_{0.02}VO_4$	2	69.92	$5.74.10^{-3}$	0.95134
(5 %) $Bi_{0.95}Ni_{0.05}VO_4$	5	84.77	$8.51.10^{-3}$	0.9466
(10 %) $Bi_{0.9}Ni_{0.1}VO_4$	10	64.61	$5.22.10^{-3}$	0.9684
(20 %) $Bi_{0.8}Ni_{0.2}VO_4$	20	55.91	$3.72.10^{-3}$	0.9848
(30 %) $Bi_{0.7}Ni_{0.3}VO_4$	30	41.41	$2.21.10^{-3}$	0.9964

As shown in Figure 6B and Table 2, the rate constant (k) for the photocatalytic degradation of MB of the catalysts (2 %) $Bi_{0.98}Ni_{0.02}VO_4$ ($k = 5.74.10^{-3}$ min^{-1}) and (5 %) $Bi_{0.95}Ni_{0.05}VO_4$ ($k= 8.51.10^{-3}$ min^{-1}) is 1.5 and 2.2 times higher than the undoped $BiVO_4$ ($k= 3.87.10^{-3}$ min^{-1}), respectively. Therefore, it can be concluded that the highest rate constant (k) and the reaction rate were obtained in the sample (5 %) $Bi_{0.95}Ni_{0.05}VO_4$.

4. CONCLUSIONS

Undoped and Ni-doped $BiVO_4$ photocatalyst materials at Bi^{3+} positions have been successfully synthesized by hydrothermal method. The XRD patterns show that the structural characteristics of all $BiVO_4$ photocatalyst materials doped with Ni metal at the Bi^{3+} site at various ratios from 2 % to 30 % Ni belong to the monoclinic-scheelite $BiVO_4$ structure. The UV-Vis method shows that the $BiVO_4$ samples and the Ni metal-doped $BiVO_4$ samples at the Bi site can both absorb light in the visible light region. The PL results show that the $BiVO_4$ material is doped with Ni metal in Bi^{3+} sites has low luminescence ability, which indicates that Ni doping would limit the electron-hole recombination phenomenon. The photocatalytic activity of undoped and Ni-doped $BiVO_4$ materials was investigated in the decomposition reaction of MB pigment under visible light. The photocatalytic activity of Ni-doped $BiVO_4$ materials is based on the change of Ni and Bi^{3+} ratios in the decolorization reaction of MB. In general, samples of Ni-doped materials (2 % - 10 %) performed well with MB color treatment efficiency above 60 %. Meanwhile, the MB processing efficiency was highest (84.77 %) in the 5 % molar Ni-doped sample, 30 % higher than the original BiVO4 sample.

Acknowledgements. This research is funded by Graduate University of Science and Technology under Grant No. GUST.STS.ĐT2020-KHVL11.

CRediT authorship contribution statement. Van Thinh Pham and Ngoc Quyen Tran: Methodology, Investigation, Funding acquisition. Bach Tuyet T. Dao: Formal analysis. Thi Kim Ngan Tran: Formal analysis, Supervision. Long Giang Bach: Formal analysis. Casen Panaitescu: Supervision. etc.

Declaration of competing interest. The authors declare that they have no known competing financial interests or personal relationships that could have appeared to influence the work reported in this paper.

REFERENCES

1. Younis S. A., Kwon E. E., Qasim M., Kim K. H., Kim T., Kukkar D., Dou X., and Ali I. - Metal-organic framework as a photocatalyst: Progress in modulation strategies and environmental/energy applications. Prog. Energy Combust. Sci., Elsevier Ltd **81** (2020) 100870. http://dx.doi.org/10.1016/j.jallcom.2014.01.130
2. Kudo A. and Miseki Y. - Heterogeneous photocatalyst materials for water splitting. Chem. Soc. Rev. **38** (2009) 253-278.
3. Malathi A., Madhavan J., Ashokkumar M., and Arunachalam P. - A review on $BiVO_4$ photocatalyst: Activity enhancement methods for solar photocatalytic applications. Appl. Catal.A Gen., Elsevier B.V.555 (2018) 47-74. http://dx.doi.org/10.1016/j.apcata. 2018.02.010
4. Nguyen D. T. and Hong S. S. - The Effect of Solvent on the Synthesis of $BiVO_4$ Using Solvothermal Method and Their Photocatalytic Activity Under Visible Light Irradiation, Top. Catal., Springer US **60** (2017) 782-788.
5. Nguyen T. D., Nguyen V. H., Nanda S., Vo D. V. N., Nguyen V. H., Van Chan T., Nong

L. X., Nguyen T. T., Bach L. G., Abdullah B., *et al*. - $BiVO_4$ photocatalysis design and applications to oxygen production and degradation of organic compounds: a review. Environ. Chem. Lett., Springer International Publishing **18** (2020) 1779-1801. https://doi.org/10.1007/s10311-020-01039-0

6. Regmi C., Kshetri Y. K., Kim T. H., Pandey R. P., Ray S. K. and Lee S. W. - Fabrication of Ni-doped $BiVO_4$ semiconductors with enhanced visible-light photocatalytic performances for wastewater treatment, Appl. Surf. Sci., Elsevier B.V. **413** (2017) 253-265.
7. Zhou B., Zhao X., Liu H., Qu J., and Huang C. P. - Synthesis of visible-light sensitive M-$BiVO_4$ (M = Ag, Co, and Ni) for the photocatalytic degradation of organic pollutants, Sep. Purif. Technol., Elsevier B.V. **77** (2011) 275-282. http://dx.doi.org/10.1016/j.seppur.2010.12.017
8. Obregón S., Caballero A. and Colón G. - Hydrothermal synthesis of $BiVO_4$: Structural and morphological influence on the photocatalytic activity, Appl. Catal. B Environ., Elsevier B.V. **117**–**118** (2012) 59-66. http://dx.doi.org/10.1016/j.apcatb.2011.12.037
9. Tan G., Zhang L., Ren H., Wei S., Huang J., and Xia A. - Effects of pH on the hierarchical structures and photocatalytic performance of $BiVO_4$ powders prepared via the microwave hydrothermal method, ACS Appl. Mater. Interfaces **5** (2013) 5186-5193.
10. Usai S., Obregón S., Becerro A. I. and Colón G. - Monoclinic-tetragonal heterostructured $BiVO_4$ by yttrium doping with improved photocatalytic activity, J. Phys. Chem. C **117** (2013) 24479-24484.
11. Kamble G. S. and Ling Y. C. - Solvothermal synthesis of facet-dependent $BiVO_4$ photocatalyst with enhanced visible-light-driven photocatalytic degradation of organic pollutant: assessment of toxicity by zebrafish embryo, Sci. Rep., Nature Publishing Group UK **10** (2020) 1-11. https://doi.org/10.1038/s41598-020-69706-4
12. Chala S., Wetchakun K., Phanichphant S., Inceesungvorn B., and Wetchakun N. - Enhanced visible-light-response photocatalytic degradation of methylene blue on Fe-loaded $BiVO_4$ photocatalyst, J. Alloys Compd., Elsevier B.V. **597** (2014) 129-135. http://dx.doi.org/10.1016/j.jallcom.2014.01.130
13. Photocatalyst B., Hunge Y. M., Uchida A., Tominaga Y., Fujii Y., Yadav A. A., Kang S., Suzuki N., Shitanda I., Kondo T., *et al.* - Visible Light-Assisted Photocatalysis Using Spherical-Shaped (2021) 1-11.
14. Zhang Z., Wang W., Shang M., and Yin W. - Photocatalytic degradation of rhodamine B and phenol by solution combustion synthesized $BiVO_4$ photocatalyst, Catal. Commun., Elsevier B.V. **11** (2010) 982-986. http://dx.doi.org/10.1016/j.catcom.2010.04.013
15. Naqvi F. K., Beg S. and Anwar K. - Synthesis of visible light active copper, iron co-doped $BiVO_4$ photocatalyst for the degradation of phenol, React. Kinet. Mech. Catal., Springer International Publishing **131** (2020) 409-422. https://doi.org/10.1007/s11144-020-01863-z
16. Qin C., Liao H., Rao F., Zhong J., and Li J. - One-pot hydrothermal preparation of Br-doped $BiVO_4$ with enhanced visible-light photocatalytic activity. Solid State Sci., Elsevier Masson SAS **105** (2020) 106285. https://doi.org/10.1016/j.solidstatesciences.2020.106285
17. Regmi C., Kshetri Y. K., Pandey R. P., Kim T. H., Gyawali G., and Lee S. W. - Understanding the multifunctionality in Cu-doped $BiVO_4$ semiconductor photocatalyst, J. Environ. Sci. (China), Elsevier B.V. **75** (2019) 84-97. https://doi.org/10.1016/j.jes.2018.03.005

18. Zhang S., Ou X., Yang X., Wang D., and Zhang C. - Preparation and properties of Al^{3+}-doped $BiVO_4$ semiconductor photocatalyst, Chem. Phys. Lett., Elsevier B.V. **778** (2021) 138747. https://doi.org/10.1016/j.cplett.2021.138747
19. Athawale A., Bokare A., Singh H., Nguyen V. H., Vo D. V. N., Kumar D., and Sharma A. - Synthesis of Ag_2O Coated TiO_2 Nanoparticles by Sonochemically Activated Methods for Enhanced Photocatalytic Activities, Top. Catal., Springer US **63** (2020) 1056-1065. https://doi.org/10.1007/s11244-020-01374-0
20. Jalalah M., Faisal M., Bouzid H., Park J. G., Al-Sayari S. A., and Ismail A. A. - Comparative study on photocatalytic performances of crystalline α- and β-Bi_2O_3 nanoparticles under visible light, J. Ind. Eng. Chem., The Korean Society of Industrial and Engineering Chemistry **30** (2015) 183-189. http://dx.doi.org/10.1016/j.jiec.2015.05.020
21. Li S., Cheng Y., Wang Q., Liu C., and Xu L. - Design, fabrication and characterization of photocatalyst Ni-doped $BiVO_4$for high effectively degrading dye contaminant, Mater. Res. Express, IOP Publishing **7** (2020).
22. Nong L. X., Nguyen V. H., Bach L. G., Tran T. V., Hong S. S., Abdullah B., Hien N. K., and Nguyen T. D. - Crystal violet degradation over $BiVO_4$ photocatalyst under visible light irradiation, Chem. Eng. Commun., Taylor & Francis **208** (2021) 530-538. https://doi.org/10.1080/00986445.2019.1674823